Conversion of 48e $Os_3(CO)_{10}$(R-DAB(4e)) via 50e $Os_3(CO)_{10}$(R-DAB(6e)) to 50e $Os_3(CO)_9$(R-DAB(8e)) (R-DAB = RN=C(H)C(H)=NR).[1] X-ray Structure of $Os_3(CO)_9$(*i*-Pr-DAB(8e)), with Two Elongated Os–Os Bonds

Robert Zoet, Gerard van Koten, Derk J. Stufkens, and Kees Vrieze*

Anorganisch Chemisch Laboratorium, University of Amsterdam, Nieuwe Achtergracht 166, 1018 WV Amsterdam, The Netherlands

Casper H. Stam

Laboratorium voor Kristallografie, University of Amsterdam, Nieuwe Achtergracht 166, 1018 WV Amsterdam, The Netherlands

Received November 24, 1987

The 48e cluster $Os_3(CO)_{10}$(*i*-Pr-DAB(4e)) (**1b**)[1b] with a chelating 4e-donating *i*-Pr-DAB ligand (abbreviated as *i*-Pr-DAB(4e)) is converted in refluxing *n*-hexane into the 50e cluster $Os_3(CO)_{10}$(*i*-Pr-DAB(6e)) (**2b**) with a bridging 6e-donating *i*-Pr-DAB ligand (abbreviated as *i*-Pr-DAB(6e)). By further heating **2b** is decarbonylated to give $Os_3(CO)_9$(*i*-Pr-DAB(8e)) (**3b**) with an 8e-donating *i*-Pr-DAB ligand (abbreviated as *i*-Pr-DAB(8e)). Under similar reaction conditions $Os_3(CO)_{10}$(c-Pr-DAB(6e)) (**2a**) reacted to give $Os_3(CO)_9$(c-Pr-DAB(8e)) (**3a**). Thermolysis of $Os_3(CO)_{10}$(neo-Pent-DAB(4e)) (**1c**) in refluxing *n*-hexane gave a complicated mixture of products from which no pure compound could be isolated. The complexes have been characterized by NMR, IR, and FD-mass spectroscopy while a single-crystal X-ray structure determination has been carried out for **3b**. Crystals of $Os_3(CO)_9$(*i*-Pr-DAB(8e)) (**3b**) are monoclinic, space group $C2/c$, with a = 31.145 (2) Å, b = 10.228 (1) Å, c = 15.429 (1) Å, β = 110.13 (1)°, and Z = 8. The structure has been solved via the heavy-atom method and refined to R = 0.041 and R_w = 0.045 using 3150 independent reflections above the 2.5$\sigma(I)$ level. The compound contains a triangular array of Os atoms with two elongated Os–Os distances [Os(1)–Os(2) = 3.0839 (7) Å and Os(2)–Os(3) = 2.9513 (7) Å] while the third Os–Os distance is shortened [Os(1)–Os(3) = 2.7969 (7) Å] when compared to the Os–Os distances in $Os_3(CO)_{12}$. The *i*-Pr-DAB ligand is σ,σ-N,N′-coordinated to Os(2) while both imine bonds are η^2-coordinated to Os(1). The latter is indicated by the equal distances between Os(1) and the C and N atoms of the flat N(1)=C(10)—C(11)=N(2) skeleton as well as the lengthened C=N and shortened C(10)—C(11) bond distances [1.390 (8) Å (mean)]. Accordingly the diimine ligand is in a symmetrical 8e-coordination mode. Electron counting shows that **3b** sould be considered as a 50e trinuclear species in which no Os–Os bond seems realy to be broken. It is shown that this structure may be interpreted by the polyhedral skeletal electron pair theory (PSEP). FTIR kinetic measurements show that, with approximately first-order kinetics, $Os_3(CO)_{10}$(*i*-Pr-DAB(4e)) (**1b**) converts to $Os_3(CO)_{10}$(*i*-Pr-DAB(6e)) (**2b**) and subsequently to $Os_3(CO)_{10}$(*i*-Pr-DAB(8e)) (**3b**).

Introduction

Part of the research in our laboratory is focused on the coordination chemistry and the chemical activation of the versatile R-DAB ligand[1b] when bonded to metal carbonyl moieties.[2a–c]

It is known that in the reaction of $Ru_3(CO)_{12}$ with R-DAB the trinuclear cluster is broken down rapidly with the formation of mononuclear Ru(CO)$_3$(R-DAB(4e)) as the first observable intermediate.[3,4] It has been shown that Ru(CO)$_3$(R-DAB(4e)) may react with $Ru_3(CO)_{12}$ to form bi-, tri-, and tetranuclear clusters. In particular the trinuclear clusters $Ru_3(CO)_n$(R-DAB(8e)) (n = 8, 9) are fascinating, since the 48e cluster $Ru_3(CO)_8$(R-DAB(8e)) could be converted reversibly with CO to the 50e cluster $Ru_3(CO)_9$(R-DAB(8e)) which contains two elongated Ru–Ru bonds and one normal one. In order to obtain more information about the intimate steps in reactions of trinuclear metal carbonyl complexes with R-DAB ligands, we directed our attention to reactions involving $Os_3(CO)_{10}(MeCN)_2$ which is known to react in a facile way with ligands, generally without rupture of the trinuclear cluster.[5]

Recently we have shown that in the room-temperature reaction of R-DAB with $Os_3(CO)_{10}(MeCN)_2$ two isomers of $Os_3(CO)_{10}$(R-DAB) were formed (see Scheme I for schematic structures).[6] In the case of the larger R groups (R = neo-Pent) one isomer, $Os_3(CO)_{10}$(neo-Pent-DAB(4e)) (**1c**), is formed with a chelating 4e-donating R-DAB ligand and a closed metal triangle with three Os–Os bonds. For smaller R groups (R = c-Pr) only $Os_3(CO)_{10}$(c-Pr-DAB(6e)) (**2a**), with a 6e-donating R-DAB ligand and only two Os–Os bonds, is isolated and not the isomer similar to **1** with the chelating R-DAB ligand. For R = *i*-Pr the type of isomer formed depended on the polarity of the solvent used in the

* To whom correspondence should be addressed.

(1) (a) Part 2. For an earlier part see ref 6. (b) 1,4-Disubstituted-1,4-diaza-1,3-dienes [R—N=C(H)—C(H)=N—R] are abbreviated as R-DAB. The number of electrons donated by the R-DAB ligand to the cluster is indicated in parentheses; i.e., R-DAB(4e) stands for σ,σ-*N,N′*-chelating, 4e coordinated; R-DAB(6e) stands for σ-N, μ_2-N′, η^2-C=N′-bridging, 6e coordinated; R-DAB(8e) stands for σ,σ-N,N′-η^2,η^2-C=N,-C′=N′-bridging, 8e coordinated.

(2) (a) van Koten, G.; Vrieze, K. *Adv. Organomet. Chem.* **1982**, *21*, 151. (b) Vrieze, K. *J. Organomet. Chem.* **1986**, *300*, 307. (c) Vrieze, K.; van Koten, G. *Inorg. Chim. Acta* **1985**, *100*, 79.

(3) Keijsper, J.; Polm, L.; van Koten, G.; Seignette, P. F. A. B.; Stam, C. H.; Vrieze, K. *Inorg. Chem.* **1985**, *24*, 518.

(4) Keijsper, J.; Polm, L.; van Koten, G.; Abbel, G.; Stam, C. H.; Vrieze, K. *Inorg. Chem.* **1984**, *23*, 2142.

(5) Deeming, A. J. *Adv. Organomet. Chem.* **1986**, *26*, 1.

(6) Part 1: Zoet, R.; Jastrzebski, J. T. B. H.; van Koten, G.; Mahabiersing, T.; Vrieze, K.; Heijdenrijk, D.; Stam, C. H. *Organometallics*, preceding paper in this issue.

(7) Staal, L. H.; van Koten, G.; Fokkens, R. H.; Nibbering, N. M. M. *Inorg. Chim. Acta* **1981**, *50*, 205.

0276-7333/88/2307-2118$01.50/0

reactions. In polar solvents, such as MeCN and THF, $Os_3(CO)_{10}$(*i*-Pr-DAB(4e)) (**1b**) is the main isomer formed while in toluene $Os_3(CO)_{10}$(*i*-Pr-DAB(6e)) (**2b**) is the most abundant product.

In view of our results on the $Ru_3(CO)_{12}$/R-DAB reaction systems (vide supra), it was of great interest to attempt to decarbonylate the two isomers of $Os_3(CO)_{10}$(R-DAB) (**1** and **2**, Scheme I) with the aim of preparing $Os_3(CO)_n$(R-DAB(8e)) (n = 8, 9).

In this paper we present an FTIR kinetic study of the intimate reaction steps in the decarbonylation reaction of $Os_3(CO)_{10}$(R-DAB) (**1b** and **1c**) with 4e-bonded R-DAB ligands and $Os_3(CO)_{10}$(R-DAB) (**2a** and **2b**) with 6e bonded R-DAB ligands, leading to $Os_3(CO)_9$(R-DAB(8e)) (Scheme I; **3a**, R = c-Pr; **3b**, R = *i*-Pr) and decomposition in the case of **1c**. Furthermore it is shown by means of a single-crystal X-ray structure determination that $Os_3(CO)_9$(*i*-Pr-DAB(8e)) has a molecular structure completely analogous to that of $Ru_3(CO)_9$(neo-Pent-DAB(8e)).

Experimental Section

Materials and Apparatus. ^1H NMR spectra were obtained on a Bruker WM250 spectrometer and ^{13}C NMR spectra on a Bruker AM 500 spectrometer. IR spectra were recorded with a Perkin-Elmer 283 spectrophotometer. Fourier transform infrared spectra (FTIR) spectra were obtained on a Nicolet 7199B FTIR interferometer (liquid-nitrogen-cooled Hg, Cd, Te detector; 32 scans, resolution = 0.5 cm^{-1}). For the high-temperature experiments a Beckman variable-temperature unit VLt-2 was used with a FH-01 VT cell and CsI windows (0.1-mm path length). Field desorption (FD) mass spectra were obtained with a Varian MAT 711 double-focussing mass spectrometer with a combined EI/FD/FI ion source and coupled to spectro system MAT 100 data aquisition unit. An emitter current between 0 and 10 mA was used to desorb the samples, the ion source temperature being 70 °C.[7] Elemental analyses were carried out by the section Elemental Analyses of the Institute of Applied Chemistry, TNO, Zeist, The Netherlands. All preparations were carried out in an atmosphere of purified nitrogen by using carefully dried solvents. Silica gel (60 mesh) for column chromatography was activated before use. The $Os_3(CO)_{10}$(R-DAB) complexes **1b**, **1c**, **2a**, and **2b** (Scheme I) have been prepared according to literature methods.[6]

Synthesis of $Os_3(CO)_9$(R-DAB(8e)) (3a, R = c-Pr; 3b, R = *i*-Pr). A solution of **1b**, **2a**, or **2b** (0.22 mmol) was refluxed for about 24 h in 100 mL of *n*-hexane or, alternatively, 8 h in *n*-heptane until the IR spectrum indicated that the ν(CO) pattern of the starting material was replaced by that of **3a** or **3b**, respectively. The color of the solution had changed from red to yellow/orange. The solvent was evaporated, and the residue was dissolved in 0.5 mL of CH_2Cl_2. The product was separated by column chromatography. The first red fraction (eluent hexane/diethyl ether = 10/1) contained some starting material while the second yellow/orange fraction (eluent hexane/diethyl ether = 2/1) contained **3a** or **3b**, respectively. The eluent containing the product was evaporated to 5 mL, and the product precipitated as crystals upon cooling to −20 °C (yield of **3a** 0.02 mmol, 10%; yield of **3b** 0.11 mmol, 50%). Anal. $C_{17}H_{16}N_2O_9Os_3$ (**3b**): C, 21.19; H, 1.66; N, 2.91. Found: C, 21.94; H, 1.72; N, 2.82.

For both **3a** and **3b** FD-mass spectra were recorded. With an emitter current of 0 mA the m/z of the molecule ion was found (highest peaks m/z 960 for **3a** and m/z 964 for **3b**). The spectra showed the typical Os_3 isotopic pattern of the molecule ion that agreed well with the simulated spectra. With an emitter current of 10 mA the parent ion of **3a** was not observed owing to decomposition. At 10 mA compound **3b** gave a mass spectrum in which only the $[M - CO]^+$ pattern was observed.

Attempted Thermolysis of $Os_3(CO)_{10}$(neo-Pent-DAB(8e)) (1c). A procedure similar to the one used above was followed. However during the reaction a dark precipitate was formed. IR spectra of both the solution and the precipitate indicated that **1c** had reacted to form a complex mixture from which no pure products could be isolated.

Attempted Synthesis of $Os_3(CO)_8$(*i*-Pr-DAB(8e)). (i) Thermolysis of $Os_3(CO)_9$(*i*-Pr-DAB(8e)) (3b). A solution of **3b** (0.11 mmol) was slowly heated from 23 to 140 °C (about 1 °C/min) in 50 mL of *n*-nonane while the reaction was monitored by taking samples for IR spectroscopy. This showed that **3b** reacted at 140 °C to form a complex mixture of products. Pure products could not be isolated.

(ii) Thermolysis Reaction of $Os_3(CO)_9$(*i*-Pr-DAB(8e)) (3b) in the Presence of Me_3NO. A solution of **3b** (0.11 mmol) and freshly sublimed Me_3NO (0.1 mmol), dissolved in 25 mL of hexane or alternatively THF, was slowly heated from 23 to 60 °C (about 1 °C/min). IR spectroscopy of the solution indicated that at 60 °C the starting material slowly decomposed.

FTIR Spectroscopy of the Conversions of 1b to 3b via 2b and of 2b to 3b. For the FTIR measurements at high temperature (323–373 K) the variable-temperature infrared cell was filled with a solution of either **1b** or **2b** in *n*-nonane. This high boiling solvent was chosen to avoid as much as possible the evaporation of the solvent during the measurements since the cell was not sealed because carbon monoxide must be able to evolve from the solution. The cell was placed in the corresponding vessel, which was flushed with nitrogen, and was heated in 15 min to the reaction temperature after which the spectra were recorded every 15 min. The temperature of the cell was kept constant within a range of 1.5 °C.

Crystal Structure Determination of $Os_3(CO)_9$(*i*-Pr-DAB(8e)) (3b) ($Os_3C_{17}H_{16}N_2O_9$; Nonacarbonyl[1,4-diisopropyl-1,4-diaza-1,3-butadiene(3*Os*–*Os*)]triosmium). Crystal data and numerical details of the structure determination are listed in Table I. X-ray data were collected on a Enraf-Nonius CAD4 diffractometer, using graphite-monochromated Cu Kα radiation. The osmium positions were derived from an E^2 Patterson synthesis. A subsequent F_o synthesis revealed the remaining nonhydrogen atoms. After isotropic block-diagonal least-squares refinement an empirical absorption correction (DIF ABS[8a]) was applied. Subsequent anisotropic refinement converged to R = 0.041 and R_w = 0.045 for the 3150 observed reflections. The anomalous dispersion of osmium was taken into account[8b] and a weighting scheme was applied. The computer programs used were from the XRAY76 system.[8c] The molecular geometry of **3b** with the numbering of the atoms is given in Figure 1, which shows an ORTEP drawing of the molecule. Atomic parameters, bond lengths, and bond angles are given in Tables II, III and IV,

Table I. Crystal Data and Details of the Structure Determination of $Os_3(CO)_9$(*i*-Pr-DAB(8e))

(a) Crystal Data	
formula	$Os_3C_{17}H_{16}N_2O_9$
mol wt	964
space group	$C2/c$
b, Å	31.145 (2)
b, Å	10.228 (1)
c, Å	15.429 (1)
β, deg	110.13 (1)
V, Å^3	4614.7 (11)
Z	8
D_{calcd}, g cm^{-3}	1.99
F(000), electrons	3456
μ(Cu Kα), cm^{-1}	309.4
cryst size, mm	0.10 × 0.15 × 0.18
(b) Data Collection	
radiatn	Cu Kα, λ = 1.5418 Å
θ_{min}, θ_{max}, deg	2.5, 65
data set	$-36 \le h \le 36$, $3 \le k \le 12$, $0 \le l \le 18$
ref reflctns	202
total data	7860
obsd data ($I > 2.5\sigma(I)$)	3150
(c) Refinement	
no. of refined parameters	280
weighting scheme	$w = 1/(6 + F_o + 0.023F_o^2)^{1/2}$
R, wR	0.041, 0.045

(8) (a) Walker, N.; Stuart, D. *Acta Crystallogr., Sect. C: Cryst. Struct. Commun.* **1983**, *A39*, 158. (b) *International Tables for Crystallography*; Kynoch: Birmingham, England, 1974; Vol. IV. (c) Stewart, J. M. *The XRAY76 system*, Technical Report TR 446; Computer Science Center, University of Maryland: College Park, MD.

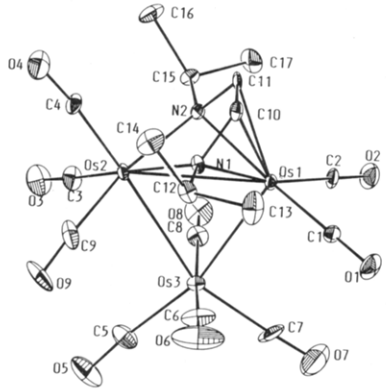

Figure 1. The molecular geometry of $Os_3(CO)_9$(*i*-Pr-DAB(8e)) (**3b**).

Table II. Fractional Coordinates with Calculated Standard Deviations in Parentheses of $Os_3(CO)_9$(*i*-Pr-DAB) (3b)

atom	*x*	*y*	*z*
Os(1)	0.07166 (2)	0.12358 (6)	0.06936 (4)
Os(2)	0.16510 (2)	0.22137 (6)	0.06805 (4)
Os(3)	0.12589 (2)	0.28350 (7)	0.21219 (4)
C(1)	0.0530 (5)	0.011 (2)	0.142 (1)
C(2)	0.0153 (5)	0.202 (2)	0.051 (1)
C(3)	0.1794 (6)	0.401 (2)	0.073 (1)
C(4)	0.1929 (6)	0.183 (2)	−0.020 (1)
C(5)	0.1737 (6)	0.395 (2)	0.290 (1)
C(6)	0.1527 (8)	0.123 (2)	0.270 (1)
C(7)	0.0817 (7)	0.278 (2)	0.274 (1)
C(8)	0.0957 (6)	0.428 (2)	0.136 (1)
C(9)	0.2209 (6)	0.192 (2)	0.167 (2)
C(10)	0.0987 (5)	0.005 (2)	−0.020 (1)
C(11)	0.0770 (4)	0.114 (1)	−0.070 (1)
C(12)	0.1633 (5)	−0.084 (1)	0.107 (1)
C(13)	0.1330 (7)	−0.193 (2)	0.130 (2)
C(14)	0.1876 (7)	−0.143 (2)	0.046 (1)
C(15)	0.0789 (5)	0.355 (1)	−0.085 (1)
C(16)	0.0947 (7)	0.350 (2)	−0.170 (1)
C(17)	0.0270 (6)	0.371 (2)	−0.117 (1)
N(1)	0.1349 (3)	0.029 (1)	0.0599 (8)
N(2)	0.0966 (4)	0.232 (1)	−0.0288 (8)
O(1)	0.0407 (5)	−0.062 (1)	0.188 (1)
O(2)	−0.0193 (4)	0.250 (1)	0.040 (1)
O(3)	0.1898 (5)	0.507 (1)	0.073 (1)
O(4)	0.2123 (5)	0.172 (1)	−0.070 (1)
O(5)	0.2002 (6)	0.460 (2)	0.341 (1)
O(6)	0.1696 (9)	0.033 (2)	0.306 (1)
O(7)	0.0554 (7)	0.277 (2)	0.306 (1)
O(8)	0.0777 (5)	0.516 (1)	0.095 (1)
O(9)	0.2530 (4)	0.180 (2)	0.230 (1)

Table III. Bond Distances of the Atoms (Å) with Standard Deviations in Parentheses of $Os_3(CO)_9$(*i*-Pr-DAB(8e)) (3b)

Os(1)–Os(2)	3.0839 (7)	C(1)–O(1)	1.178 (15)
Os(1)–Os(3)	2.7969 (7)	C(2)–O(2)	1.141 (14)
Os(1)–C(1)	1.843 (12)	C(3)–O(3)	1.130 (15)
Os(1)–C(2)	1.861 (11)	C(4)–O(4)	1.137 (18)
Os(1)–C(10)	2.209 (11)	C(5)–O(5)	1.140 (19)
Os(1)–C(11)	2.208 (10)	C(6)–O(6)	1.110 (21)
Os(1)–N(1)	2.243 (8)	C(7)–O(7)	1.097 (22)
Os(1)–N(2)	2.222 (8)	C(8)–O(8)	1.133 (15)
Os(2)–Os(3)	2.9513 (7)	C(9)–O(9)	1.135 (19)
Os(2)–C(3)	1.889 (11)	C(10)–C(11)	1.394 (15)
Os(2)–C(4)	1.886 (13)	C(10)–N(1)	1.378 (14)
Os(2)–C(9)	1.903 (15)	C(11)–N(2)	1.398 (14)
Os(2)–N(1)	2.163 (8)	C(12)–C(13)	1.571 (19)
Os(2)–N(2)	2.145 (8)	C(12)–C(14)	1.531 (19)
Os(3)–C(5)	1.931 (14)	C(12)–N(1)	1.489 (14)
Os(3)–C(6)	1.917 (15)	C(15)–C(16)	1.548 (18)
Os(3)–C(7)	1.927 (16)	C(15)–C(17)	1.527 (18)
Os(3)–C(8)	1.919 (12)	C(15)–N(2)	1.520 (13)

respectively. A stereo ORTEP drawing and all anisotropic thermal parameters and a list of observed and calculated structure factors are included within the supplementary material.

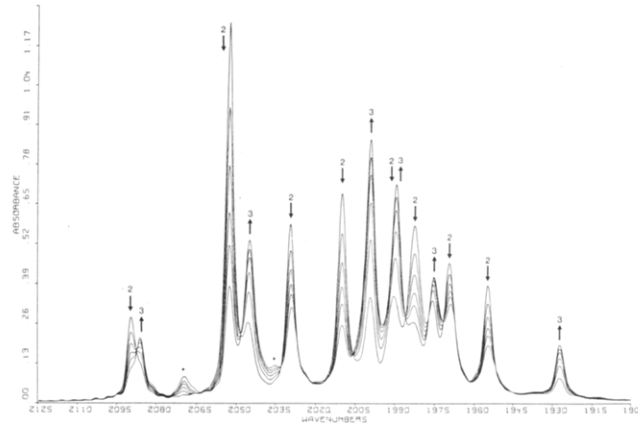

Figure 2. The thermolysis reaction of $Os_3(CO)_{10}$(*i*-Pr-DAB(6e)) (**2b**) at 80 °C in *n*-nonane followed with FTIR spectroscopy at time intervals of 15 min. Bands marked with an asterisk are assigned to $Os_3(CO)_{12}$.

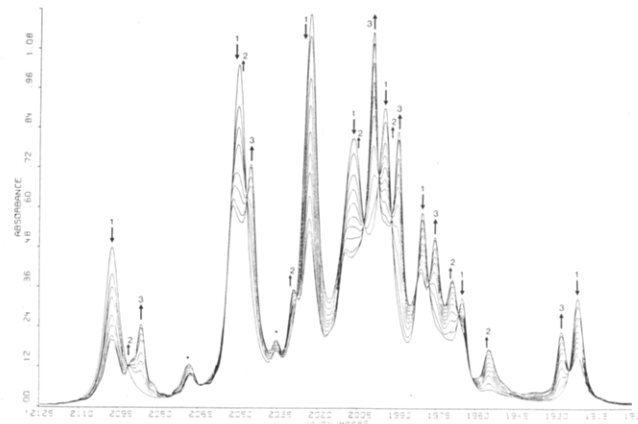

Figure 3. The thermolysis reaction of $Os_3(CO)_{10}$(*i*-Pr-DAB(4e)) (**1b**) in *n*-nonane at 70 °C followed with FTIR spectroscopy at time intervals of 60 min. Bands marked with an asterisk are assigned to $Os_3(CO)_{12}$.

Results

Formation of Products. Thermolysis of a solution of the 48e cluster $Os_3(CO)_{10}$(*i*-Pr-DAB(4e)) (**1b**), with a σ,σ-N,N′-chelating, 4e-donating *i*-Pr-DAB ligand, in refluxing hexane or heptane afforded $Os_3(CO)_9$(*i*-Pr-DAB(8e)) (**3b**), containing an 8e-donating R-DAB ligand (see Scheme I). Under the same reaction conditions 50e $Os_3(CO)_{10}$(R-DAB(6e)) (**2a**, R = c-Pr, **2b**, R = *i*-Pr), with a σ-N, μ_2-N′, η^2-C=N′-bridging, 6e-donating R-DAB ligand, was decarbonylated to give $Os_3(CO)_9$(R-DAB(8e)) (**3a**, R = c-Pr; **3b**, R = *i*-Pr). Thermolysis of $Os_3(CO)_{10}$(neo-Pent-DAB-(4e)) (**1c**) yielded a complex mixture of products from which no pure compound could be isolated. At several temperatures the thermolysis reactions of **1b** as well as that of separately prepared **2b** were followed with FTIR spectroscopy by monitoring the intensity changes of the characteristic ν(CO) absorptions for **1b** (1921 cm^{-1}), **2b** (1955 cm^{-1}), and **3b** (1927 cm^{-1}).

When the reaction of **2b** is followed in the temperature range 70–90 °C, one observes in all cases a smooth disappearance of the bands of the starting complex and a concomitant increase of the intensities of the bands of **3b** together with those of the decomposition product $Os_3(CO)_{12}$ (see Figure 2 for the reaction at 80 °C). The reaction was found to be first order with the concentration of **2b**.

When the reaction of **1b** is followed at several temperatures between 70 °C and 90 °C, a more complicated process was observed (see Figure 3 for the reaction at 70

Table IV. Bond Angles of the Atoms (deg) with Standard Deviations in Parentheses of $Os_3(CO)_9$(*i*-Pr-DAB) (3b)

Os(2)–Os(1)–Os(3)	60.01 (3)	Os(1)–Os(3)–Os(2)	64.83 (3)
Os(2)–Os(1)–C(1)	134.8 (4)	Os(1)–Os(3)–C(5)	164.4 (4)
Os(2)–Os(1)–C(2)	134.5 (4)	Os(1)–Os(3)–C(6)	85.1 (6)
Os(2)–Os(1)–C(10)	67.2 (4)	Os(1)–Os(3)–C(7)	91.8 (6)
Os(2)–Os(1)–C(11)	67.7 (3)	Os(1)–Os(3)–C(8)	86.0 (5)
Os(2)–Os(1)–N(1)	44.52 (24)	Os(2)–Os(3)–C(5)	99.6 (6)
Os(2)–Os(1)–N(2)	44.07 (24)	Os(2)–Os(3)–C(6)	86.6 (7)
Os(3)–Os(1)–C(1)	96.7 (5)	Os(2)–Os(3)–C(7)	156.6 (4)
Os(3)–Os(1)–C(2)	98.6 (5)	Os(2)–Os(3)–C(8)	86.9 (5)
Os(3)–Os(1)–C(10)	123.8 (3)	C(5)–Os(3)–C(6)	95.4 (9)
Os(3)–Os(1)–C(11)	124.3 (3)	C(5)–Os(3)–C(7)	103.8 (9)
Os(3)–Os(1)–N(1)	89.8 (3)	C(5)–Os(3)–C(8)	92.4 (8)
Os(3)–Os(1)–N(2)	89.3 (3)	C(6)–Os(3)–C(7)	90.8 (10)
C(1)–Os(1)–C(2)	83.4 (8)	C(6)–Os(3)–C(8)	170.6 (7)
C(1)–Os(1)–C(10)	107.7 (7)	C(7)–Os(3)–C(8)	92.5 (9)
C(1)–Os(1)–C(11)	135.4 (5)	Os(1)–C(1)–O(1)	179.2 (9)
C(1)–Os(1)–N(1)	103.9 (6)	Os(1)–C(2)–O(2)	179.5 (8)
C(1)–Os(1)–N(2)	171.2 (5)	Os(2)–C(3)–O(3)	176.1 (9)
C(2)–Os(1)–C(10)	133.2 (5)	Os(2)–C(4)–O(4)	172.5 (10)
C(2)–Os(1)–C(11)	104.6 (6)	Os(3)–C(5)–O(5)	174.6 (11)
C(2)–Os(1)–N(1)	168.3 (5)	Os(3)–C(6)–O(6)	177.5 (12)
C(2)–Os(1)–N(2)	102.2 (6)	Os(3)–C(7)–O(7)	177.1 (13)
C(10)–Os(1)–C(11)	36.8 (4)	Os(3)–C(8)–O(8)	176.5 (9)
C(10)–Os(1)–N(1)	36.0 (4)	Os(2)–C(9)–O(9)	175.4 (11)
C(10)–Os(1)–N(2)	63.4 (5)	Os(1)–C(10)–C(11)	71.6 (9)
C(11)–Os(1)–N(1)	63.7 (4)	Os(1)–C(10)–N(1)	73.3 (9)
C(11)–Os(1)–N(2)	36.8 (4)	C(11)–C(10)–N(1)	115.9 (11)
N(1)–Os(1)–N(2)	69.5 (4)	Os(1)–C(11)–C(10)	71.7 (9)
Os(1)–Os(2)–Os(3)	55.16 (3)	Os(1)–C(11)–N(2)	72.1 (8)
Os(1)–Os(2)–C(3)	121.8 (5)	C(10)–C(11)–N(2)	113.1 (13)
Os(1)–Os(2)–C(4)	127.2 (5)	C(13)–C(12)–C(14)	109.0 (15)
Os(1)–Os(2)–C(9)	123.1 (5)	C(13)–C(12)–N(1)	111.1 (13)
Os(1)–Os(2)–N(1)	46.65 (25)	C(14)–C(12)–N(1)	109.5 (13)
Os(1)–Os(2)–N(2)	46.1 (3)	C(16)–C(15)–C(17)	109.9 (14)
Os(3)–Os(2)–C(3)	85.2 (6)	C(16)–C(15)–N(2)	107.2 (12)
Os(3)–Os(2)–C(4)	177.3 (4)	C(17)–C(15)–N(2)	114.3 (11)
Os(3)–Os(2)–C(9)	85.8 (6)	Os(1)–N(1)–Os(2)	88.8 (4)
Os(3)–Os(2)–N(1)	87.4 (3)	Os(1)–N(1)–C(10)	70.6 (8)
Os(3)–Os(2)–N(2)	86.8 (3)	Os(1)–N(1)–C(12)	133.5 (7)
C(3)–Os(2)–C(4)	94.0 (8)	Os(2)–N(1)–C(10)	115.1 (8)
C(3)–Os(2)–C(9)	89.1 (8)	Os(2)–N(1)–C(12)	120.5 (7)
C(3)–Os(2)–N(1)	168.3 (5)	C(10)–N(1)–C(12)	117.5 (11)
C(3)–Os(2)–N(2)	98.2 (7)	Os(1)–N(2)–Os(2)	89.8 (5)
C(4)–Os(2)–C(9)	91.7 (9)	Os(1)–N(2)–C(11)	71.1 (8)
C(4)–Os(2)–N(1)	93.8 (7)	Os(1)–N(2)–C(15)	131.2 (7)
C(4)–Os(2)–N(2)	95.9 (8)	Os(2)–N(2)–C(11)	116.4 (7)
C(9)–Os(2)–N(1)	99.3 (7)	Os(2)–N(2)–C(15)	121.2 (7)
C(9)–Os(2)–N(2)	169.1 (6)	C(11)–N(2)–C(15)	116.1 (11)
N(1)–Os(2)–N(2)	72.4 (4)		

°C). The starting complex **1b** reacts to form **2b**, **3b**, and $Os_3(CO)_{12}$ by a reaction that is first order with the concentration of **1b**. A careful examination of the 1965–1900 cm^{-1} region (see Figure 4) shows that in the early stages of the reaction the intensity decrease in the 1921 cm^{-1} band of **1b** is accompanied solely by a simultaneous increase in the 1955 cm^{-1} band of **2b** (first spectrum of Figure 4) while only in the later stages the formation of **3b** becomes evident from the appearance of its characteristic 1927 cm^{-1} band. From this it may be concluded that **3b** is not directly formed from **1b** but only via **2b**. The conversion of **2b** to **3b** at 70 °C (and higher) is understandable in view of the above observation that **2b** is thermally unstable at this temperature and converts into **3b** and some $Os_3(CO)_{12}$. Unfortunately, a quantitative kinetic analysis of the thermolysis reactions was prevented by the partial decomposition of the parent compounds.

Several attempts have been made to decarbonylate **3b** to form $Os_3(CO)_8$(*i*-Pr-DAB(8e)). A solution of **3b** in *n*-nonane reacted at 140 °C to form a complex mixture of products from which no pure products could be isolated. Also IR spectroscopy did not give any indication of the formation $Os_3(CO)_8$(*i*-Pr-DAB(8e)). Finally, a solution of **3b** was reacted with Me_3NO that resulted, however, only

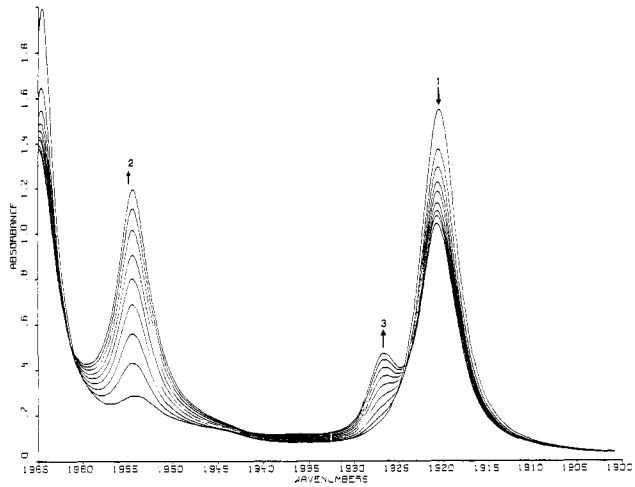

Figure 4. Closer inspection of the 1965–1900 cm^{-1} region of the thermolysis reaction of $Os_3(CO)_{10}$(*i*-Pr-DAB(4e)) (**1b**) in *n*-nonane at 70 °C and time intervals of 15 min (see also Figure 3).

in the decomposition of **3b** when a temperature of 60 °C was reached.

Molecular Geometry of $Os_3(CO)_9$(*i*-Pr-DAB(8e)) (3b). The molecular geometry of **3b** together with the atomic numbering is given in Figure 1. In Tables III and IV the bond lengths and angles are given.

The molecule contains a triangular array of Os atoms with two elongated Os–Os distances, Os(1)–Os(2) = 3.0839 (7) Å and Os(2)–Os(3) = 2.9513(7) Å, while the third one, Os(1)–Os(3) = 2.7969 (7) Å, is shortened when compared with the normal single Os–Os bond found in $Os_3(CO)_{12}$ (2.8871 (27) Å (mean).[9] Of the nine terminally bonded carbonyls in **3b** two are bonded to Os(1), three to Os(2), and four to Os(3). The geometry around Os(1) is not well-defined. When the Os(1)–Os(2) vector is neglected, Os(2) is approximately octahedrally surrounded by N(1), N(2), C(3), C(4), C(9), and Os(3). Os(3) has a distorted octahedral coordination while the structural features of the $Os(3)(CO)_4$ unit are closely related to that of the three $Os(CO)_4$ units in $Os_3(CO)_{12}$. The average Os(1)–C(O) bond length of 1.852 (8) Å (mean) and the Os(2)–C(O) of 1.893 (7) Å (mean) are rather short, whereas the average Os(3)–C(O) bond length [1.924 (7) Å (mean)] is similar to that of $Os_3(CO)_{12}$ [$Os_3(CO)_{12}$: Os–C(O)(axial) = 1.946 (6) Å (mean) and Os–C(O)(equatorial) = 1.912 (7) Å (mean)]. It must be noted that when carbonyls are substituted for electron-donating ligands, a shortening of the remaining M–C(O) bond lengths is commonly observed which explains the relative short Os(1)–C(O) and Os(2)–C(O) bonds in the present complex.

The Os(1)–Os(2) bond is bridged by the $Os(3)(CO)_4$ unit and by the *i*-Pr-DAB ligand which has the structural characteristics of an 8e-donating σ,σ-N,N′-η^2,η^2-C=N,-C′=N′ coordination mode.[2a-c,3,4,10] The two Os(2)–N distances are 2.163 (8) and 2.145 (8) Å for Os(2)–N(1) and Os(2)–N(2), respectively. Indicative for the η^2,η^2-C=N,-C′=N′ coordination are the long N=C distances for C(10)–N(1) and C(11)–N(2) of 1.378 (14) and 1.398 (14) Å, respectively, and the shortened central C(10)–C(11) bond length of 1.394 (15) Å. The bond angles of about 115° around the imine N and imine C atoms and the equal distances of the atoms of the NCCN skeleton to Os(1) [Os(1)–N(1) = 2.243 (8) Å, Os(1)–N(2) = 2.222 (8) Å, Os(1)–C(10) = 2.209 (11) Å, and Os(1)–C(11) = 2.208 (10) Å]

(9) Churchill, M. R.; DeBoer, B. G. *Inorg. Chem.* **1977**, *16*, 878.
(10) Muller, F.; van Koten, G.; Vrieze, K., to be submitted for publication.

Table V. Spectroscopic Data

compd	ν(CO)[a]	^{1}H and ^{13}C NMR chem shifts[b]		
			R group	imine
$Os_3(CO)_9$(c-Pr-DAB(8e)) (**3a**)	2082, 2044, 2000, 1989, 1977, 1925	^{1}H[c]	0.89 (m, 4 H); 1.19 (m, 4 H); 2.26 (m, 2 H)	4.41 (s, 2 H)
$Os_3(CO)_9$(i-Pr-DAB(8e)) (**3b**)	2087, 2046, 1999, 1990, 1976, 1927	^{1}H[c]	0.67 (d, 6 Hz, 6 H)/ 0.90 (d, 6 Hz, 6 H), 3.26 (sept, 6 Hz, 2 H)	4.60 (s, 2 H)
		^{13}C[d]	17.9/23.8; 57.6	91.0

[a] In hexane solution (cm^{-1}). [b] Shifts are in ppm relative to TMS; vertical bars separate diastereotropic pairs; abbreviations: d, doublet; s, singlet; m, multiplet; sept, septet. [c] In benzene-d_6, 250 MHz. [d] In dichloromethane-d_2, 125.77 MHz.

are in agreement with the 8e-coordination mode of the *i*-Pr-DAB ligand. The extensive C=N bond lengthening and C(10)—C(11) bond shortening is due to the π-back-bonding from Os(1) into the LUMO of the diimine, which is antibonding between C and N and bonding between the central C atoms C(10) and C(11).[2a-c,6,11]

NMR Spectroscopy. The ^{1}H and ^{13}C NMR data are listed in Table V.

In the ^{1}H NMR spectra the imine protons of $Os_3(CO)_9$(c-Pr-DAB(8e)) (**3a**) and $Os_3(CO)_9$(*i*-Pr-DAB(8e)) (**3b**) appear as one singlet at about 4.5 ppm. In the ^{13}C NMR spectrum of **3b** the imine carbons give a single resonance at 91.0 ppm. These ^{1}H and ^{13}C chemical shift values for the imine protons and carbon atoms, respectively, of **3a** and **3b** are upfield compared to those of the free ligand values and lie in the range normally observed for 8e-donating R-DAB ligands.[2a-c] For example the imine protons of the 8e-donating R-DAB ligands in $Ru_3(CO)_8(\mu\text{-}CH_2)$(neo-Pent-DAB(8e)),[12] $Ru_3(CO)_9$(R-DAB(8e)),[3] and $Ru_2(CO)_5$(R-DAB(8e))[4] resonate at 6.3, 5.3, and 6.0 ppm, respectively, while the imine carbons of $Ru_3(CO)_8(\mu\text{-}CH_2)$(neo-Pent-DAB(8e)) resonate at 102.9 ppm. As expected the resonances of the imine protons and carbon atoms of the osmium compounds **3a** and **3b** are upfield as compared to those observed for the ruthenium compounds. The c-Pr and *i*-Pr groups of **3a** and **3b** give rise to single patterns, again indicating that the R-DAB ligand is in a symmetrical coordination mode.

Discussion

Structure. The NMR data and the single-crystal X-ray structure determination of **3b** show that the *i*-Pr-DAB ligand acts as an 8e donor ligand. It is further shown that two Os–Os distances are elongated. It follows from electron counting that the cluster core of **3b** contains 50 electrons and that Os(2) has a formal electron count of 20 electrons, assuming three single 2e–2c Os–Os bonds and σ,σ-N,N′ coordination of R-DAB to Os(2).

Before discussing the relation between the electron count and the geometry of **3b**, it seems worthwhile to devote some discussion to the question whether in **3b** a true Os–Os bond is present between Os(1) and Os(2). For example, for the 50e cluster $Os_3(CO)_{10}(OMe)_2$ it was concluded that there are two Os–Os bonds while the third OMe-bridged Os–Os distance of 3.078 (3) Å was considered as nonbonding.[14] In contrast, for the 50e cluster [PPN][$Os_3(CO)_{10}(\mu\text{-}CH_2)(\mu\text{-}I)$] (a bridged Os–Os distance of 3.112 (1) Å) it was concluded from the geometry around the bridging CH_2 and I ligands that there is an Os–Os interaction.[15] The selective lengthening of Os–Os bonds observed for **3b** is not unprecedented. The 64e clusters $Os_4(CO)_{12}(\mu_3\text{-}S)_2$ and $WOs_3(CO)_{12}(PMe_2Ph)(\mu_3\text{-}S)_2$ contain five metal–metal interactions instead of the expected four.[16,17] For the former compound two Os–Os bonds are lengthened to 3.091 (1) and 3.002 (1) Å, and for the latter compound Os–Os and Os–W distances of 3.060 (1) and 3.031 (1) Å, respectively, have been found.

The metal–metal bond lengths of **3b** may be compared with those of $Ru_3(CO)_9$(c-Hex-DAB(8e)) and $Ru_3(CO)_8$(neo-Pent-DAB(8e)).[3,13] In $Ru_3(CO)_9$(c-Hex-DAB(8e)), which is isostructural and isoelectronic with **3b**, a similar pattern of metal–metal distances has been observed as in **3b** [two elongated distances Ru(1)–Ru(2) = 3.026 (1) Å and Ru(2)–Ru(3) = 2.956 (1) Å and one single bond distance Ru(1)–Ru(3) = 2.793 (1) Å]. The observation that this contrasts with the three single Ru–Ru bonds observed for $Ru_3(CO)_8$(neo-Pent-DAB(8e)), which is an 48e species since it contains only eight carbonyl ligands and an 8e-donating neo-Pent-DAB ligand, shows that there are three Ru–Ru interactions in $Ru_3(CO)_9$(c-Hex-DAB(8e)).

From these examples and the observation that in **3b** besides the Os(1)–Os(2) bond the Os(2)–Os(3) bond is also lengthened, it follows from our view that a considerable interaction still exists between Os(1) and Os(2).

Several theories have been developed to describe clusters that do not obey the 18e rule.[18a-d] For **3b** the polyhedral skeletal electron pair (PSEP) theory can be used to relate the geometry of **3b** with the stoichiometry.[19a-c] Starting from the hypothetical $Os_3(CO)_8$(R-DAB(8e)) and treating the C(H) and N(R) units of the ligand as 3e and 4e contributing vertices, this is a nido-type cluster. It is based on a pentagonal bipyramid of which one edge is bridged by an $Os(CO)_4$ unit and which contains eight skeletal electron pairs. Addition of the ninth CO gives the arachno-type cluster $Os_3(CO)_9$(R-DAB(8e)) based on a dodecahedron containing nine skeletal electron pairs. The same theory was applied for $Ru_3(CO)_9$(c-Hex-DAB(8e)).[3] However, in spite of the fact that in this way the relation between the electron count and the geometry of **3b** can be explained, this theory does not account for the selective

(11) Vrieze, K.; van Koten, G.; Keijsper, J.; Stam, C. H. *Polyhedron* **1983**, *2*, 1111.
(12) Keijsper, J.; Polm, L. H.; van Koten, G.; Vrieze, K.; Goubitz, K.; Stam, C. H. *Organometallics* **1985**, *4*, 1876.
(13) Polm, L.; van Koten, G.; Vrieze, K., to be submitted for publication.
(14) Allen, V. F.; Mason, R.; Hitchcock, P. B. *J. Organomet. Chem.* **1977**, *140*, 297.
(15) Geoffroy, G. L.; Morrison, E. D. *Organometallics* **1985**, *4*, 1413.
(16) Adams, R. D.; Yang, L.-W.; *J. Am. Chem. Soc.* **1983**, *105*, 235.
(17) Adams, R. D.; Horváth, I. T.; Mathur, P. *J. Am. Chem. Soc.* **1984**, *106*, 6296.
(18) (a) Teo, B. *Inorg. Chem.* **1984**, *23*, 1251. (b) King, R. B. *Inorg. Chim. Acta* **1986**, *116*, 99. (c) Wade, K. In *Transition Metal Clusters*; Johnson, B. F. G., Ed.; Wiley: New York, 1980. (d) Lauher, J. W. *J. Organomet. Chem.* **1981**, *213*, 25.
(19) (a) Adams, R. D.; Horváth, I. T.; Mathur, P. *Organometallics* **1984**, *3*, 623. (b) Adams, R. D.; Horváth, I. T.; Mathur, P.; Segmüller, B. E.; Yang, L. W. *Organometallics* **1983**, *2*, 1078. (c) Adams, R. D.; Yang, L. W. *J. Am. Chem. Soc.* **1982**, *104*, 4115.

Scheme I. Proposed Pathway for the Conversion of $Os_3(CO)_{10}$(*i*-Pr-DAB(4e)) (1b) to $Os_3(CO)_{10}$(*i*-Pr-DAB(6e)) (2b) and Further to $Os_3(CO)_9$(*i*-Pr-DAB(8e)) (3b)

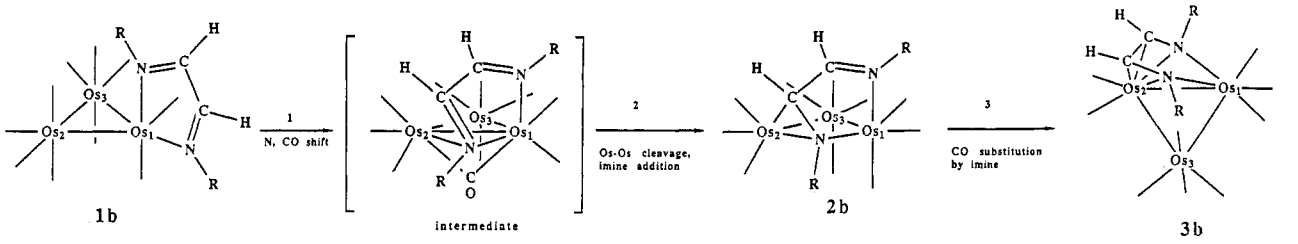

lengthening of the Os(1)–Os(2) and Os(2)–Os(3) bonds. As a rationalization for this observation it seems most likely that in **3b** three Os–Os bonds are present but that two of them are weakened through the occupation of a low-lying LUMO comprising mainly the Os(1)–Os(2) and Os(2)–Os(3) bonds by two electrons.

Reaction Pathway for the Formation of 3b. As we could isolate both **1b** and **2b**, it was possible to follow the thermolysis reactions of both compounds with FTIR spectroscopy. These measurements showed that when **2b** was used as starting material, this compound converted at temperatures between 70 °C and 90 °C to **3b** (see Results). When **1b** was heated at temperatures between 70 °C and 90 °C, **2b** was formed first. Subsequently the production of **3b** was observed. The mechanism we propose for this reaction is depicted in Scheme I together with a schematic representation of the structures of **1b**, **2b**, and **3b**. The former two structures, with *i*-Pr-DAB ligands that are bonded via 4e and 6e, respectively, are described in detail elsewhere.[6] It is significant that the distribution of carbonyl ligands among the three osmium atoms Os(1), Os(2), and Os(3) in complex **1b** is 2, 4, and 4; in complex **2b** is 3, 3, and 4; and in complex **3b** is 3, 2, and 4, respectively (Scheme I). Apparently during the conversion of **1b** to **2b** a carbonyl group is shifted from Os(2) to Os(1), an imine bond is coordinated to Os(2), and the Os(1)–Os(2) bond is ruptured. For the first step of this conversion we therefore propose that one carbonyl ligand bonded to Os(2) and a nitrogen bonded to Os(1) shift simultaneously to bridging positions (intermediate in Scheme I).[20] The second step could be the formation of a coordinatively unsaturated cluster with a ruptured Os(1)–Os(2) bond.[21a–c] Subsequently one geometrically close imine group of the R-DAB ligand attacks the Os(2) atom which gives **2b**.[22] In the reaction of **2b** to **3b** (and the reaction of **2a** to **3a**) one carbonyl ligand on Os(2) is substituted by the second, noncoordinated, imine bond together with the re-formation of an interaction between Os(1) and Os(2) (Scheme I).

Interestingly only decomposition was observed in the thermolysis reaction of **1c**. A possible explanation for this might be that the neo-Pent-DAB ligand has a relatively large R group as compared to c-Pr and *i*-Pr which makes it less suited to act as a 6e or 8e donor ligand in the case of osmium. This behavior may be compared with the reaction of $Os_3(CO)_{10}(MeCN)_2$ with neo-Pent-DAB to $Os_3(CO)_{10}$(neo-Pent-DAB(4e)) which only gives **1c** with a σ,σ-N,N′-chelating neo-Pent-DAB ligand and not the isomer with the 6e-donating neo-Pent-DAB ligand.

Finally, it is of interest to compare the thermolysis behavior of $Os_3(CO)_9$(*i*-Pr-DAB(8e)) (**3b**) with that of $Ru_3(CO)_9$(R-DAB(8e)). It has been found that in refluxing toluene $Ru_3(CO)_9$(R-DAB(8e)) easily looses one carbonyl ligand to form $Ru_3(CO)_8$(R-DAB(8e)) and that the reaction is reversible.[3] Complex **3b**, however, converts at 140 °C in nonane into a complex mixture of products from which no pure product could be isolated. This difference in reactivity between $Ru_3(CO)_9$(R-DAB(8e)) and **3b** might be rationalized by the greater kinetic stability of the osmium compound **3b** compared to the ruthenium compound $Ru_3(CO)_9$(R-DAB(8e)) with respect to decarbonylation. At the higher reaction temperatures needed for the simple decarbonylation of **3b** other reactions may start to dominate, thereby hindering the formation of $Os_3(CO)_8$(*i*-Pr-DAB(8e)). In an attempt to circumvent this problem **3b** was also reacted with Me_3NO, which, however, led only to decomposition and not to an isolable amount of $Os_3(CO)_8$(*i*-Pr-DAB(8e)).

Acknowledgment. We thank G. C. Schoemaker for his assistance in recording the FTIR spectra and E. Kluft and G. U. A. Sai for recording the mass spectra. We thank Dr. C. J. Elsevier and Dr. H. W. Frühauf for fruitful discussions. We thank the Netherlands Foundation for Chemical Research (S.O.N.) and the Netherlands Organisation for Pure Research (Z.W.O.) for their financial support.

Registry No. **1b**, 115160-80-0; **2a**, 115160-81-1; **2b**, 115160-82-2; **3a**, 115185-62-1; **3b**, 115160-83-3; Os, 7440-04-2.

Supplementary Material Available: A listing of anisotropic thermal parameters of the non-hydrogen atoms and a stereo ORTEP view for **3b** (2 pages); a listing of structure factor amplitude (14 pages). Ordering information is given on any current masthead page.

(20) A similar shift has been proposed by Adams et al. in the reaction of $H_2Os_3(CO)_9(P(CH_3)_2C_6H_5)$ with CS_2 which gave $HOs_3(\mu\text{-}SCH_2)(CO)_9(P(CH_3)_2C_6H_5)$. Adams, R. D.; Golembeski, N. M.; Selegue, J. P. *J. Am. Chem. Soc.* **1981**, *103*, 546.

(21) (a) Johnson, B. F. G. *Inorg. Chim. Acta* **1986**, *115*, L39. (b) Lewis, J.; Johnson, B. F. G. *Gazz. Chim. Ital.* **1979**, *109*, 271. (c) Johnson, B. F. G.; Lewis, J.; Pippard, D. *J. Organomet. Chem.* **1978**, *160*, 263.

(22) Metal–metal bond cleavage in osmium cluster chemistry induced by the addition of electron-donating ligands is a generally observed phenomenon. Albers, M. O.; Robinson, D. J. *Coord. Chem. Rev.* **1986**, *69*, 127. Mays, M. J.; Raithby, P. R.; Dawoodi, Z. *J. Chem. Soc., Chem. Commun.* **1979**, 721. Dawoodi, Z.; Mays, M. J. *J. Chem. Soc., Dalton Trans.* **1984**, 1931 and ref 16.